Final Draft

of the original manuscript

Kyzyma, O.; Mchedlov-Petrossyan, N.; Al-Shuuchi, Y.; Tropin, T.; Ivankov, O.; Kriklya, N.; Gromovoy, T.; Kryshtal, A.; Zhigunov, A.; Korosteleva, E.; Shekhovtsov, S.; Garamus, V.; Bulavin, L.:

Diluted and concentrated organosols of fullerene C60 in the toluene–acetonitrile solvent system as studied by diverse experimental methods.

DILUTED AND CONCENTRATED ORGANOSOLS OF FULLERENE C_{60} IN THE TOLUENE–ACETONITRILE SOLVENT SYSTEM AS STUDIED BY DIVERSE EXPERIMENTAL METHODS

Olena A. Kyzyma, [a,b] N. O. Mchedlov-Petrossyan,[c*] Y. Turki Mahmood Al-Shuuchi,[d] Timur V. Tropin, [b] Oleksandr I. Ivankov, [b,e,f] N. N. Kriklya,[c] T. Yu. Gromovoy,[g] A. P. Kryshtal,[h] Alexander N. Zhigunov,[i]

E. A. Korosteleva,[j] S. V. Shekhovtsov,[c] Vasil M.Garamus,[k] L. A. Bulavin[a]

[a] *Taras Shevchenko National University of Kyiv, 64/13 Volodymyrska St., Kyiv 01601, Ukraine.* [b]*Frank Laboratory of Neutron Physics, Joint Institute for Nuclear Research, Joliot-Curie St. 6, 141980 Dubna, Moscow Reg., Russia.* [c]*Department of Physical Chemistry, V. N. Karazin National University, 61022, Kharkov, Ukraine .*[d]*Department of Chemistry, College of Education for Pure Sciences, University of Mosul, Mosul, Iraq.* [e] *Institute for Safety Problems of Nuclear Power Plants, NAS Ukraine, Kiev, Ukraine.* [f] *Moscow Institute of Physics and Technology, Dolgoprudny, Russia.* [g] *A. A. Chuiko Institute of Surface Chemistry, National Academy of Sciences of Ukraine, 03164, Kiev, Ukraine.* [h] *AGH University of Science and Technology, International Centre of Electron Microscopy for Material Science and Faculty of Metals Engineering and Industrial Computer Science, al. A.Mickiewicza, 30-059 Kraków, Poland.* [i] *Institute of Macromolecular Chemistry AS CR, v.v.i., Heyrovskeho nam. 2,162 06, Czech Republic.* [j] *Pharmstandart-Biolik, 61084, Kharkov, Ukraine.* [k] *Helmholtz-Zentrum Geesthacht: Centre for Materials and Coastal Research, Max-Planck-Street 1, 21502 Geesthacht, Germany*

* Corresponding author
mchedlov@karazin.ua

ABSTRACT

In this article, we examined the state of fullerene C_{60} in toluene and its mixtures with acetonitrile in both diluted, $(4.0$ to $6.3)\times10^{-6}$ M, and concentrated, $(0.23$ to $1.9)\times10^{-3}$ M solutions, prepared by either equilibrium or non-equilibrium procedures. Normally, the working solutions were prepared by diluting stock solutions of fullerene in toluene. Some specific features of solid fullerene interaction with atmospheric oxygen were revealed using the LDI mass-spectrometry. A combination of electron absorption spectra of the fullerene in $C_6H_5CH_3$–CH_3CN mixtures with the analysis of the particle size distribution using the DLS method demonstrated that even in acetonitrile-rich media, where diluted C_{60} exists in colloidal state, some features of the molecular absorption spectra are still present. Such effect is in line with the formation of the large solvation shells of an aromatic solvent around fullerenes. The TEM images of the dried colloidal solutions demonstrate a loose floc configuration of the aggregates, contrary to the crystal structure of the species in a toluene-free C_{60} dispersion obtained by hand-grinding. In solution, the spectrum of the last-named is a monotonous curve increasing towards ultraviolet. The LDI measurements proved the tendency of C_{60} towards forming negative species under contact with acetonitrile. Electrophoretic studies state that a universal property of the negatively charged colloidal species is their expressed ability to overcharging in the presence of inorganic cations, which are poorly solvated by acetonitrile. In concentrated (oversaturated) fullerene solutions, where the SAXS and SANS methods are applicable, fractal-type aggregates of fullerenes were revealed in solutions. The analysis of aggregates structure indicates that their packing density is increased with growth of fullerene concentration and/or amount of acetonitrile in the mixture. Thus, branched aggregates were observed in toluene solution, while fullerenes form dense clusters with diffusive surface in mixtures with acetonitrile.

1. Introduction

Presently, the fullerenes belong to the most widely used compounds. Their numerous utilizations in academic and applied science, nanotechnologies, medicine, etc., are well known. One of the notable features of fullerenes is their very limited solubility in liquids. Even in the so-called good, i.e., aromatic non-polar solvents and CS_2, the solubility reaches only $0.01 - 0.07$ M (hereafter, 1 M = 1 mol dm^{-3}) [1–3]. Another typical feature is the ability to form colloidal solutions in "poor" (polar) solvents. They readily appear when small volumes of C_{60} or C_{70} solutions in good solvents are mixed with larger amounts of polar ones [3–12]. Despite a series of publications devoted to the gradual transition of the fullerenes from molecular to colloidal state [5–8, 11, 13, 14], this issue needs additional research. For instance, it was shown that not only the content of the binary solvent but also the fullerene concentration influences the character of the systems of interest [4–9, 14, 15].

In this article, we use a complex of experimental methods, which allows shedding additional light upon the properties of fullerene C_{60} in the toluene–acetonitrile system. Some of the used methods are better suited for low fullerene concentrations, whereas others are applicable for concentrated solutions. In both cases, some features of large C_{60} aggregates are disclosed.

2. Experimental

2.1. Materials

Fullerene C_{60} samples from Acros Organics (purity 99.9%) and Fullerene Technologies, Russia (purity > 99.5%) were used. High purity solvents were additionally purified and dehydrated using conventional procedures. Inorganic salts were of analytical grade. The cryptand [2.2.2], or Kryptofix 222 (for synthesis), was from Merck.

2.2. Procedure of C_{60} solution preparation

For studying diluted solutions of C_{60}, two procedures were used, both without stirring and sonication. First of all, the solid material fullerene was stored in toluene for two weeks in the dark. Then, after saturation, the solution was filtrated using the 0.45 μm -pore PTFE filters. As it was previously reported, such procedure allows estimating the C_{60} solubility of fullerene as 3.8×10^{-3} M [14]. Alternatively, the procedure was the same, but the weighed amount of C_{60} was much smaller, and the saturated solution was not reached. Also, no filtration was used in this case. In such way, a solution with a concentration of 6.00×10^{-4} M was obtained.

Some experiments were made with the C_{60} colloidal solution in acetonitrile, prepared using Deguchi's procedure [16]. After hand-grinding in an agate mortar, the solid sample was placed into acetonitrile and sonicated with electrical power ca. 50 W and frequency 40 kHz; the details including the characterization of the disperse system were published previously [17].

For studying concentrated (oversaturated) solutions of C_{60}, three types of the initial fullerene C_{60} solutions in toluene were prepared. Solution I with concentration 3.8×10^{-3} M and Solution II with concentration 4.58×10^{-4} M were prepared by stirring in the vial for 1 h at room temperature under natural light. Solution III with concentration of 5.5×10^{-4} M was also obtained by stirring for 1 h at room temperature, but in the dark. Then the solutions were diluted in such a way that the fullerene concentration in all samples was the same and two times less than the initial one, and the ratios between toluene and acetonitrile varied from 7:3 to 1:1. One more C_{60} solution in toluene was prepared by plain dilution with toluene of each initial solution. Thus, all solutions had the same concentration, which made it possible to neglect the effect of concentration on aggregation processes. Synchrotron small-angle X-ray scattering (SAXS) measurements of the samples based on Solution I were carried out 7 hours after sample preparation. This time is enough for the formation of aggregates in solutions. The

samples based on Solution II were studied by small-angle neutron scattering (SANS) after 24 hours. In the case of the time evolution small-angle X-ray scattering studies the measurements were started 5 minutes after sample preparation.

2.3. UV-visible absorption

The electronic absorption spectra were run using a Hitachi U-2000 apparatus against solvent blanks.

2.4. Dynamic and static light scattering

The particle size distribution was determined via dynamic light scattering (DLS) using Zetasizer Nano ZS Malvern Instruments apparatus at 25 $^{\circ}$C, scattering angle 173° and by static light scattering (SLS) method using the laser diffraction particle size analyzer SALD-7100 Shimadzu instrument. Electrokinetic potential was also determined with the Zetasizer Nano ZS. Alternatively, the measurements of the size distribution of fullerene aggregates at higher concentrations were performed using DLS (Photocor Compact-Z, Moscow, Russia) according to ISO 22412:2017. This DLS instrument is equipped with a thermostabilized diode laser (wavelength 650 nm, maximum output power 35 mW) and covers the particle size range from 0.5 nm to 10 μm. The measurements were made at a scattering angle of 90°. The autocorrelation function of the scattered light intensity was analyzed using the DynaLS software. The temperature was 20 $^{\circ}$C for all measurements.

2.5. LDI mass spectra

Mass spectra of Laser Desorption/Ionization Time of Flight (LDI-ToF) mass spectrometry were acquired using an Autoflex II Bruker Daltonics mass spectrometer equipped with nitrogen laser of $\lambda = 337$ nm with a pulse width of 3 ns. The samples of C_{60} solutions deposited onto either a standard steel target or a teflon support, and dried under

ambient conditions. Each LDI-ToF mass spectrum was a sum of 120 individual spectra. The analyzer was operated in linear positive and negative modes.

2.6. TEM studies

Samples for transmission electron microscopy (TEM) studies were produced by drop-casting and drying C_{60} solutions on a standard copper TEM grid covered with ≈ 15 nm thick amorphous carbon film. Morphology of the samples was studied with FEI Tecnai G2 20 TWIN (LaB6, 200kV) transmission electron microscope in a bright-field mode.

2.7. Synchrotron SAXS measurements

Synchrotron SAXS measurements were performed at the P12 BioSAXS beamline at PETRA III ring (EMBL/DESY) in Hamburg, Germany. The sample-to-detector distance, 3.1 m, gave the q-range of $0.07 - 4.6$ nm^{-1} calibrated using silver behenate [18]. Scattering patterns were obtained with a Pilatus 2M pixel detector. The samples were placed into the glass capillary (1 mm of diameter). The temperature was 20 ± 0.1 °C. Twenty consecutive frames (each 0.05 s) comprising the measurement of samples and buffer were performed. In order to verify that no artifacts as a result of radiation damage occurred, all scattering curves of a recorded dataset were compared to a reference measurement (typically the first exposure) and finally integrated by automated acquisition program [19]. A signal from pure buffer was measured before and after each SAXS measurement. This signal was subtracted from a corresponding sample curve. The resulting data was normalized to the transmitted beam. For estimation of the clusters size in the fullerene systems, the SAXS curves were processed using indirect Fourier transformation (IFT) approach developed by Glatter [20] in the version of Pedersen [21].

2.8. SANS measurements

SANS measurements were carried out at the YuMO small-angle diffractometer at the IBR-2 pulsed reactor (JINR, Dubna, Russia) in the time-of-flight regime. On the YuMO small-angle spectrometer, the two-detector setup with ring wire detectors was used [22]. The neutron wavelength range was $0.05 - 0.8$ nm. The measured scattering curves were corrected for background scattering from buffer solutions. For an absolute calibration of the scattering intensity during the measurements, a vanadium standard was used. Treatment of the raw data was performed by the SAS program with a smoothing mode enabled [23].

2.9. Time evolution SAXS experiments

Time evolution small-angle X-ray scattering measurements were used to determine the nanostructure of the samples based on the Solution III. Samples were sealed in a capillaries made of borosilicate glass of 2 mm diameter (Hilgenberg GmbH, Germany). A scattering from the empty capillary was subtracted. The experiments were performed using a pinhole "Molecular Metrology" camera (Rigaku, Japan) attached to a microfocused X-ray beam generator (Rigaku MicroMax 003) operated at 50 kV and 0.6 mA (30 W). The setup was upgraded by SAXSLAB enabling the freedom in sample-to-detector position and wide q-range coverage. The scattering vector, q, is defined as $q = (4\pi/\lambda)sin\theta$, where $\lambda = 1.54$ Å is the radiation wavelength and 2θ is the scattering angle. The camera was equipped with a vacuum compatible version of Pilatus3 R 300K hybrid photon-counting detector. The typical exposure time used was 7200 seconds with the frame length 15 seconds. This gave us an opportunity to follow the changes within chosen intervals.

3. Results and discussion

3.1. Electron absorption spectra of diluted C_{60} solutions: neat toluene solvent

First, the absorption spectrum of C_{60} in pure toluene should be considered (Figure 1). Precise values of the molar absorptivity, $M^{-1} cm^{-1}$, are as follows: 58.43×10^3 (at $\lambda = 336$ nm); 3.163×10^3 (407 nm); 0.867×10^3 (526 nm); and 0.750×10^3 (565 nm); the average uncertainty is 3.4%. In *o*-xylene, the maximum is also at 336 nm (molar absorptivity 50.6×10^3) [24], while in *n*-hexane $\lambda_{max} = 327$ nm (51×10^3) [25].

The spectra obey the Bouguer–Lambert–Beer law in the used concentration range. It can be considered as a proof of absence of aggregate formation. Hence, the diluted solutions below the solubility limit may be considered as common molecular liquids. However, a series of publications by Ginzburg, Tuĭchiev, and associates [26, 27] should be taken into account. With the help of a variety of experimental methods they demonstrated that in aromatic solvents, such as benzene, toluene, and xylenes, the C_{60} and C_{70} molecules are surrounded by shells consisting of thousands of solvent molecules. This, in turn, influences the properties of the solvent in the solution [28–30] and is in concert with the substantially negative values of entropy of fullerenes solubility and solvation [3, 31]. Application of molecular dynamics simulations for fullerene C_{60} and its derivatives in a set of aromatic solvents allows revealing the formation of substantial solvation shells [32], though this method may not account the long-ranged interactions.
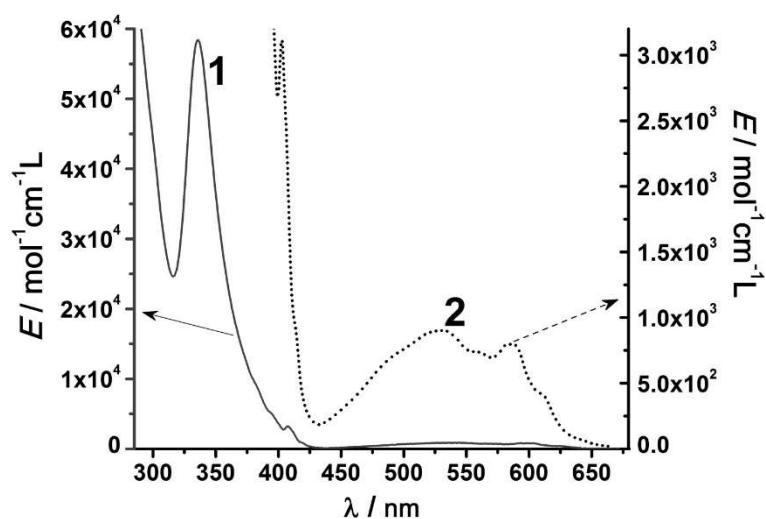
Figure 1. Absorption spectra of C_{60} in pure toluene. Fullerene concentration 6.26×10^{-6} M (1) and 6.00×10^{-4} M (2), 20 °C.

[**Figure 1** near here]

Some recent data on C_{60} solutions in *o*-xylene are in line with this concept [33]. Also, the well-known ability of fullerenes to form crystal solvates [3] including $C_{60}\bullet2C_6H_5CH_3$ [34] gives an (indirect) support of the above-mentioned ideas of stable solvate shells formation in solution. Aggregates of C_{60} in toluene and chlorobenzene were observed by Guo et al. [35] when studying solutions prepared using sonication. A number of articles, which describe fullerene aggregates in good solvents, were previously discussed in a review paper [3]. As it was demonstrated by Avdeev et al. [36], such systems appear if non-equilibrium methods of preparation were used.

Recently, Makhmanov et al. studied fullerene solutions prepared in toluene by both equilibrium and strongly non-equilibrium methods [37]. In the last case, HRTEM technique allowed observing 380 ± 20 nm nanoporous fractal structures. In the first case, however, aggregates were also observed though of smaller size (no more than 50 nm and densely-packed). It should be noted that the authors provide no information concerning the filtration of the solutions; the high absorbance values hinder the comparison of the electronic spectra with ours. Similar results were obtained with C_{70} in benzene [38] and toluene [39]. These authors also studied the coating of surfaces with fullerene C_{60} using solutions in toluene–tetrahydrofuran [40] and xylene–tetrahydrofuran [41]. It should be noted, however, that the DLS studies were made only for the last-named system, where large aggregates were revealed as in solution prepared by a non-equilibrium method. Some authors mention, that aggregates observed by TEM are formed during the evaporation of the solvent [42].

On the other hand, the formation of unstable C_{60} aggregates in benzene was reported as early as 1994 [43]. These aggregates spontaneously appear after keeping in benzene over a

month in nitrogen atmosphere without any mixing, agitation, or sonication, but may be easily destroyed by hand-shaking [43]. The SANS method also demonstrated some time-dependent aggregation during storing in toluene at concentrations close to the solubility limit [44]. Some other examples were collected in a previous review [3]. Therefore, formation of such unstable aggregates reflects the initial stage of fullerene dissolution, before even slight mixing. In contrast, the spectrum presented in Figure 1 refers to an equilibrated solution prepared following accepted analytical procedures.

3.2. LDI-Tof studies of C_{60} in toluene

Fullerene films are often used in different technological procedures [39–41]. Therefore, we examined the properties of such films using the LDI-ToF method. Data concerning the mass-spectrometry of fullerenes including the MALDI- and LDI-ToF methods are available in the literature [45–48]. The peculiarity of our study consisted in using C_{60} films on supports of two different natures exposed for a long period of time in the atmosphere. As result, some interesting features of their interaction with oxygen were revealed.

Two identical liquid samples of C_{60} solution in toluene were placed on two standard ground steel MALDI target plates, protected from dust and the direct sunlight. After 4-days exposure on air, the dried sample on one of the plates was analyzed by the LDI-ToF. At the same time, the second sample was completely washed by toluene and again put on a standard steel plate. In this case, the mass spectra were obtained just after evaporation of the toluene solution. The analyzer was operated in linear positive and negative modes in linear regimes. The thickness of the C_{60} layers on the plates corresponded on the average to ~20–30 molecules. The films were non-uniform, and some grains were observed using an optical microscope.

Analysis of negative ions of the first sample showed the increasing of C_{60} fragmentation, which manifests itself by appearance of ions at m/z 696 (C_{58}), 672 (C_{56}), 648 (C_{54}), and a series of peaks that correspond mainly to products of interaction with oxygen at m/z 709 ($C_{59}H_1$), 712 ($C_{58}O$), 720 (C_{60}), 728 ($C_{58}O_2$), 736 ($C_{60}O$), 737 ($C_{60}OH$), 740 ($C_{59}O_2$), 744 ($C_{58}O_3$), 754 ($C_{60}O_2H$), and 769 ($C_{60}O_3$).
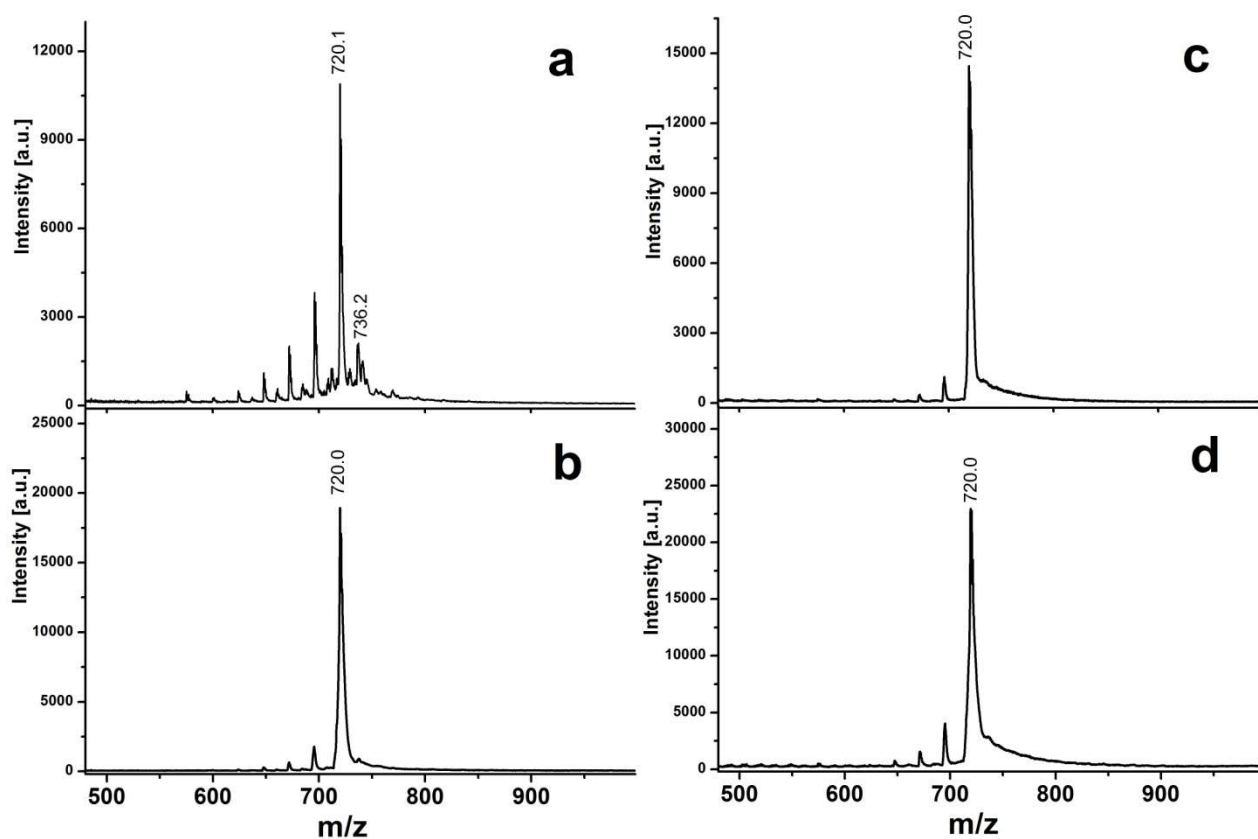

Figure 2. LDI-ToF mass spectra of negative (a, b) and positive (c, d) ions of fullerene C_{60} on a standard steel MALDI target plates obtained after 96-h exposure under ambient conditions (a, c) and after washing by toluene and placing again on a standard steel plate (b, d).

[**Figure 2** near here]

By contrast, the analysis of the second sample demonstrated the signals of fullerene destruction at m/z 696 (C_{58}) and 672 (C_{56}). Of the products of interaction with oxygen peaks, only one at 736 ($C_{60}O$) was observed, and even that possessed a lower relative intensity. This reflects the tendency of a decrease in the content of oxidized fullerene species after washing and re-placing on the steel support.

In the region of higher m/z values, in the mass spectrum of the first sample a series of peaks appear in increments of 24 Da at m/z 1272, 1296, 1320, 1344, 1368, 1392, and 1416, which corresponds the clusterized products with mass divisible by 106, 108, 110, 112, 114, 116, and 118 carbon atoms.

The peculiarity of the mass spectrum of the second sample consists in the presence of a peak at m/z 1428, which corresponds to a cluster of 119 carbon atoms [49, 50]. Peaks at m/z 1320, 1344, 1368, 1392, and 1416 are also present.

The mass spectra of the positive ions of both samples are qualitatively similar. The fragmentation process is more expressed in the second case.

For comparison, a toluene solution of C_{60} was placed on a handmade teflon plate. After 4 day-exposition on air, the plate was placed into the working zone of mass spectrometer. The analyzer was operated in positive and negative modes in linear regime. In both cases, only a peak at m/z 720 (C_{60}) was observed, with neither fragmentation nor products of interaction with oxygen.

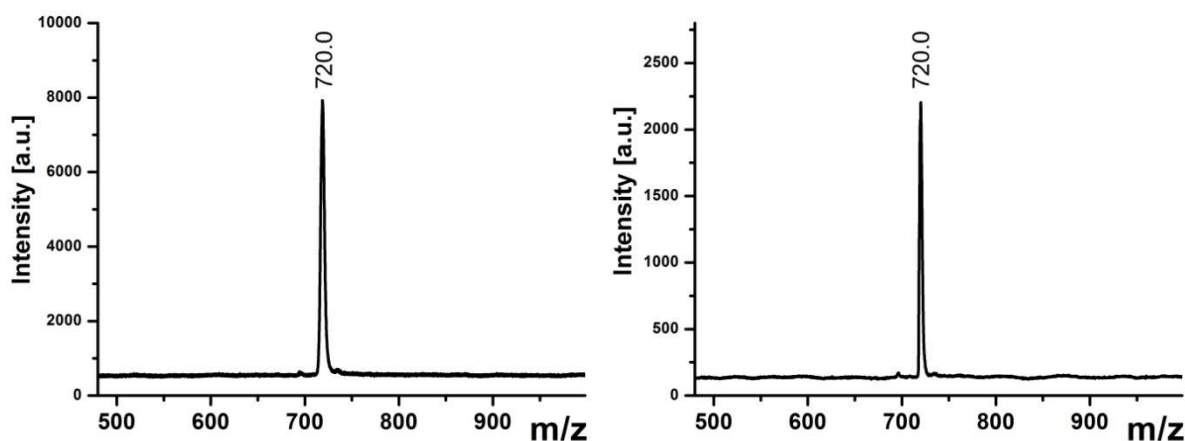All the above experiments were repeated several times.

Figure 3. LDI-ToF mass spectra of negative (left-hand) and positive (right-hand) ions of fullerene C_{60} on a standard teflon plate.

[**Figure 3** near here]

The oxidation products, in particular $C_{60}O$ are common impurity in fullerene samples [3, 51–53]. The content of these contaminations may be different in various samples and may reach several percent [3, 4–53]. Also, the use of different analytical methods can give different oxygen content in one and the same sample [52]. The concentration of $C_{60}O$ can be firmly determined in toluene extracts from aqueous colloidal solution using both HPLC method and UV-visible spectra [53] and in solid phase deposited from such hydrosols using MALDI-ToF mass spectrometry [54].

Taylor et al. assert that the most stable oxidation product of C_{60} is $C_{120}O$ [53]. Their mass-spectrometric and HPLC studies were devoted also to the formation of $(C_{70})_2O_n$ in the gas-phase aggregation [56] and to related problems [57, 58].

Irrespective of the composition of the oxides, it is very likely that they are the ones that form films on the flasks, less-soluble in toluene than the entire fullerene [55, 59]. The partial oxidation of C_{60} was observed simply on standing in air [55]. The more expressed slow aggregation of the fullerene in toluene on air as compared with that in the nitrogen atmosphere [44] should obviously be attributed to oxidation. Also, it was shown that exposure

of C_{60} solution in toluene to the light under ambient laboratory conditions leads to formation of the $C_{60}O_n$ epoxides (n = 1, 2, 3) which, in turn, induce the formation of fullerene aggregates [60]. Such aggregates are unstable with respect to heating and shaking [60]. In any case, in the spectrum of our fullerene sample in toluene the band 424–426 nm, typical for the [6,6]-closed [61] and [5,6]-open $C_{60}O$ [62], is absent (Figure 1). Hence, the fraction of the admixtures of this type in our C_{60} sample is small, in line with the LDI data except the results obtained after prolonged exposure under the laboratory atmosphere.

Our cyclic experiments with the attaching oxygen and washing-off it in toluene looked as a kind of "breathing". Hence, the results demonstrate the role of the metal support in oxygen addition to the C_{60} molecule as a result of prolonged exposure. Also, the bound is probably of non-covalent nature, because the attached oxygen atom is lost after dissolution in toluene. Though the fullerene oxides are less toluene-soluble, it seems unlikely that they were deposited in the flask after washing; no signs of sediment were observed. A kind of donor-acceptor interaction seems to be more probable. On the dielectric teflon support, oxidation products were not observed in the present study.

3.3. Diluted C_{60} solutions in toluene–acetonitrile mixed solvent

In Figure 4a, the changes of the absorption spectrum of C_{60} is shown on going from toluene (relative permittivity ε_r = 2.38) to acetonitrile (ε_r = 35.94). The picture is typical for formation of colloidal particles and resembles those for C_{60} in mixtures of toluene with methanol [14] and benzene with acetonitrile [13, 15]. In these publications, the role of the solution mixing sequence and the problem of kinetics of formation and ageing of the colloidal system were discussed. Figure 2b demonstrates that if toluene solution of C_{60} is mixed with a solvent of medium polarity, such as dichloromethane (ε_r = 8.93), no principal changes of the spectra occur. (All ε_r values are from ref. [63].)
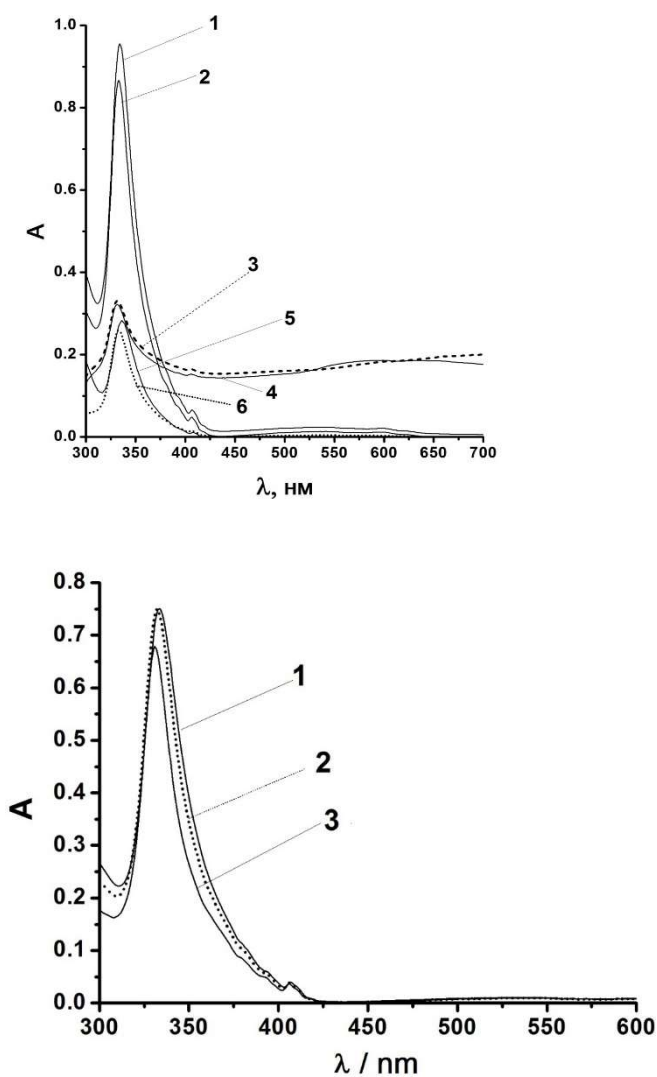
Figure 4. Absorption spectra of 4×10^{-6} M C_{60} solutions: a) in toluene–acetonitrile binary solvent at toluene content: 70 vol. % (1,2); 50 vol. % (3, 4); and 30 vol. % (5, 6); prepared by dilution of the saturated C_{60} solution in toluene (1, 3, 5) or from the 4×10^{-4} M solution of C_{60} in toluene; b) in toluene–dichloromethane binary solvent at toluene content, vol. %:70 (1); 50 (2); and 30 (3). Optical path length: 1.00 cm, 25 °C.

[**Figure 1** near here]

Figure 4a needs some comments. Beck and Mándi [64] reported following values of C_{60} solubility in toluene–acetonitrile binary solvent: 2.5×10^{-5} M (30 vol. % toluene); 4.3×10^{-5} M

(50 vol. % toluene); 9.3×10^{-5} M (60 vol. % toluene); and 4.2×10^{-4} M (80 vol. % toluene). Hence, all these saturated solutions are in fact colloidal systems; e.g., see Figure 5. This means that some interaction between C_{60} and toluene still takes place even if the fullerene molecules constitute the colloidal particles.
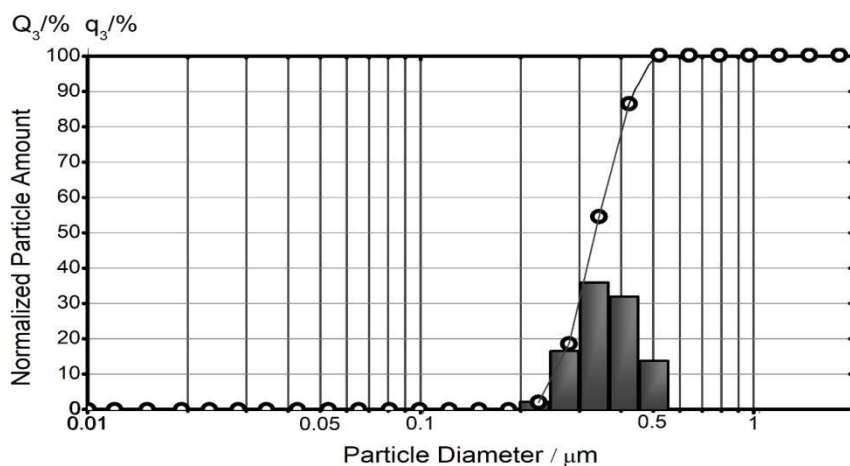

Figure 5. The SLS data for C_{60} in toluene–acetonitrile binary solvent with 30 vol % toluene.

[**Figure 5** near here]

The behavior of C_{60} and C_{70} in the toluene – acetonitrile system was a matter of detailed studies by two research groups. Sun et al. [5–7] rapidly added acetonitrile to fullerene solution in toluene. The higher the fullerene concentration is, the lower the acetonitrile content causing spectral changes is. At 5×10^{-6} M C_{60} in 70 vol. % acetonitrile, the absorption spectrum is as in neat toluene [7]. This contradicts to some extent our data (Figure 4a); the main reason may be the different preparation procedure of the solutions. In general, however, the observations by Sun et al. agree with the regularities of formation of colloidal particles formulated by Volmer [14, 65]: the lower the solubility in the given mixed solvent is, the smaller the colloidal particles are. The same can be said about the study by Alargova et al. [9], where toluene solutions of fullerenes were 200-fold diluted by acetonitrile: the higher the fullerenes C_{60} or C_{70} concentration in toluene is, the larger the colloidal species are formed in acetonitrile. This

is also in line with our data [15]: even if an almost saturated solution in toluene is 1000-fold diluted by CH_3CN, the size of the species is around 350–370 nm, whereas 100-fold dilution of a 4×10^{-6} M C_{60} resulted in much smaller 150–200 nm particles. These results were confirmed in the present study. Our studies of C_{60} in toluene–methanol [14] and benzene–acetonitrile [13] and C_{70} in toluene–acetonitrile [66] also follow the same rules. In order to fix the turning-point from molecules to colloids, some authors examined the long wavelengths portion of the visible spectra [7, 8, 14]. In general, it can be stated that the solvent composition corresponding to the above transition depends on the fullerene concentration.

The cited papers and our studies allow making an important conclusion: the main absorption band around 336 nm is observed even if the DLS data reveal colloidal species of fullerenes. Even in 99 % acetonitrile or methanol and 1 % toluene, the corresponding band is distinctly observable, though the λ_{max} values are 349 nm and 353–357 nm, respectively [14, 15, 67, 68]. Such feature of the molecular absorption allows expecting that some toluene molecules are still surrounding the fullerene molecules even in colloid species. Rudaglevi et al. [4] report a value of fractal dimension of 2.9 for C_{60} aggregates in acetonitrile with 10 % toluene and assume close packing of hard spheres. In this connection, the TEM images of the dried colloid of C_{60} in acetonitrile with 1 vol. % toluene should be compared with analogous picture obtained for the dispersion prepared using the Deguchi's method [17]. This method consists in hand-grinding of the solid sample and sonicating thus prepared solid in acetonitrile [16].

Figure 6 shows typical morphology of the species in the dispersions prepared by 100-fold dilution of C_{60} solution in toluene (A) and hand-grinding (B) on amorphous carbon substrate. It is seen that colloids prepared by condensation of C_{60} molecules primarily dissolved in toluene form a loose floc configuration with no distinct crystalline structure.

Individual particles are not resolved even at the edge of the floc supposing that it is a pile of C_{60} fullerene molecules.
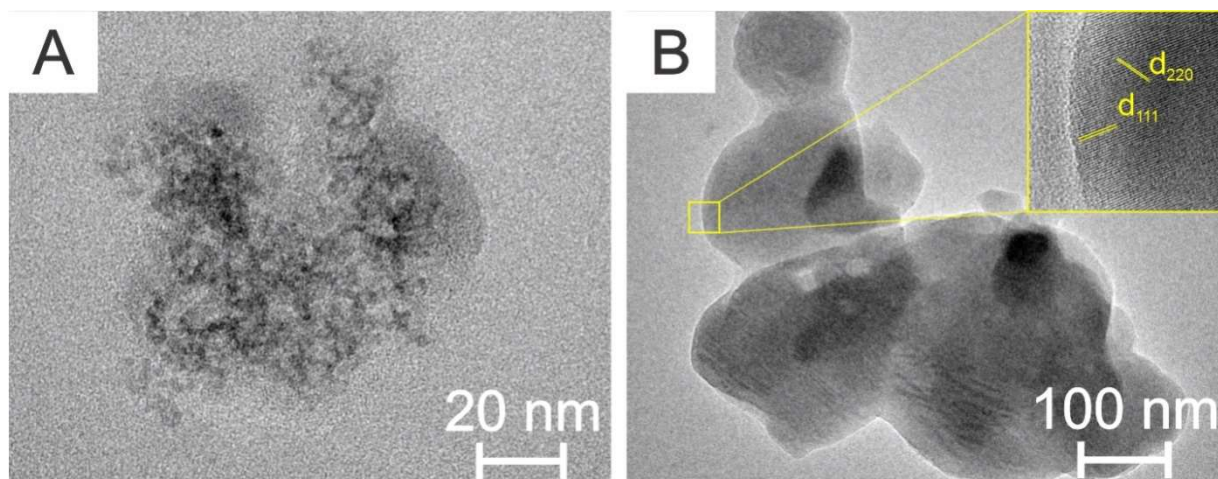

Figure 6. Bright-field TEM images of colloid (a) and hand-grinding (b) C_{60} samples. Insert in (b) shows marked area at higher magnification, revealing (111) and (220) planes of C_{60} crystal.

[**Figure 6** near here]

In contrast to the colloid prepared by dilution of fullerene solution in toluene, the sample prepared via hand-grinding method contains particles with a size of tens to hundreds nanometers. These particles are crystalline as follows from specific diffraction contrast in low-magnification image and direct resolution of crystal planes at the particle edge (inset in Figure 6b). The measured interplane distances of 0.8, 0.5 and 0.42 nm correlate well with (111), (220) and (311) planes of C_{60} fcc crystal, respectively.

The UV-visible spectra also demonstrate the difference between the two samples, while the particle sizes are quite similar (Figure 7).
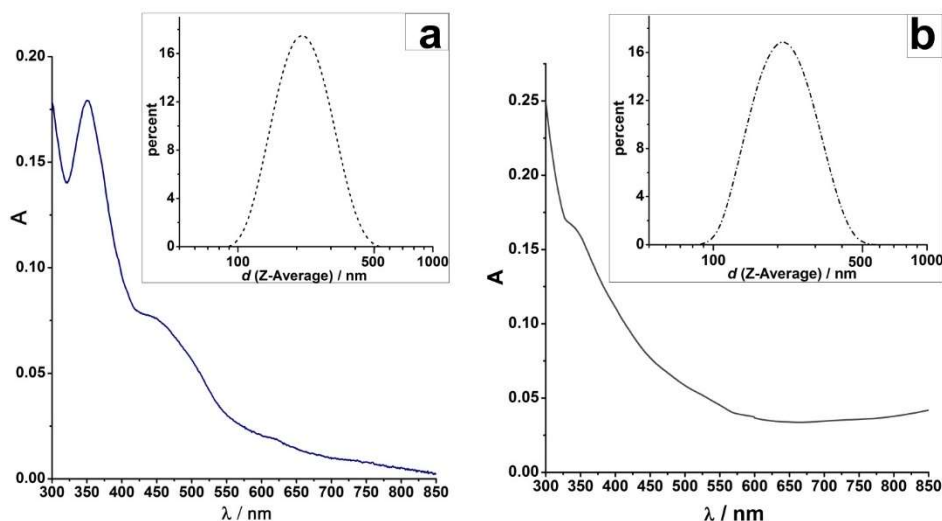
Figure 7. Absorption spectra of fullerene C_{60} (4×10^{-6} M) in acetonitrile with 1 vol % toluene, obtained by dilution of the initial 4×10^{-4} M stock solution in toluene (a); fullerene solution in acetonitrile obtained by hand-grinding method, followed by 4-h sonication with intervals (b). Inserts: size distribution of species expressed as Z-average of the solution using DLS; PDI = 0.173±0.023 (a); PDI = 0.219±0.012.

[**Figure 7** near here]

3.4. Electrical properties of colloidal particles in solution

Our LDI-ToF mass-spectrometrical experiments of the mixtures of C_{60} toluene solutions with acetonitrile indicate the expressed tendency to form negatively charged species. In this case, the intensities of the signals of latter are manifold higher as compared with those of the positively charged ions. Previously some evidence was obtained of anion-radical $C_{60}{}^{\bullet-}$ formation using ESI spectra and a radical scavenger [13, 15]. Rather quickly the more stable forms, e.g., $C_{60}{}^{2-}$ or $(C_{60})^{2-}$ probably appear. This behavior is in line with the electrokinetic potential (zeta-potential) of the colloidal C_{60} species; the particles are negatively charged with

$\varsigma = -(47-53)$ mV. The ς values were calculated basing on the electrophoretic mobility and using the Ohshima equation [69].
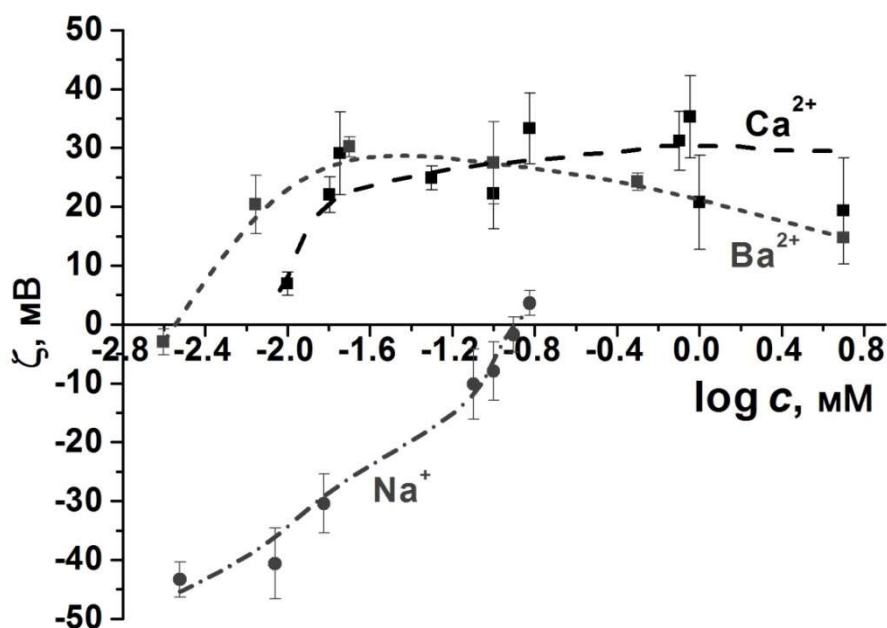

Figure 8. Overcharging of colloidal particles of C_{60} in acetonitrile (with 1 vol % toluene) by metal cations introduced in the form as perchlorates; fullerene concentration 4×10^{-6} M.

[**Figure 8** near here]

The coagulation of the organosols of C_{60} was a matter of a series of previous studies [13, 65, 66]. A specific feature of the fullerene is their ability to overcharging. In Figure 8, the corresponding data are presented. The size of colloidal species is relatively large, whereas the $|\varsigma|$ value is not very high at extremely low (but not exactly known) ionic strength. Hence, the surface charge density of the particles is low, and the metal cations that are poorly solvated in acetonitrile interact with the practically isolated negative charges. Introduction of the cryptand [2.2.2] substantially suppress the overcharging, evidently owing to form the corresponding metal cryptates, which are better solvated in acetonitrile.

As for kinetics of fullerene aggregation and cluster growth in mixtures of good and polar solvents, the reader is referred to a recent paper [70].

3.5. Structural organization of oversaturated C$_{60}$ solutions in toluene and in toluene–acetonitrile mixtures by SAXS

As it was shown previously, fullerenes can form aggregates in non-polar solvents [35, 37, 71]. It was suggested that the main reasons for this effect are the non-equilibrium methods of fullerene solutions preparation [42] and exposure to light [60]. As expected, the stock solution I, obtained by stirring under natural light, shows the presence of fullerene aggregates. The small-angle X-ray scattering (SAXS) curve of the stock solution I (inset of Figure 9) clearly demonstrates the two scattering levels. This is an indication of formation of two populations (by size) of the fullerene clusters. Previously, Guo et al. [35] revealed a similar coexistence of molecular fullerenes and their aggregates in toluene and chlorobenzene by analysis of the combined static light scattering (SLS) and SAXS intensity profiles. Also, the presence of bi-modal cluster distribution in toluene was registered by SAXS in [44, 72] and by SLS with DLS in [60]. The radius of gyration value, Rg, for each scattering level was obtained directly from a SAXS curve (inset of Figure 9) using a classical Guinier approximation [73]. Thus, the values of 11±1 nm for population of small-sized aggregates and 45±1 nm for the other population were obtained. Assuming particles to have quasispherical shapes in solution, as it was shown in [35] the radius of corresponding spheres, R, can be estimated using the well-known relation $Rg^2 = 0.6 \, R^2$ and are of about 14 nm and 58 nm, correspondingly, that is in fairly good agreement with previous reports [35, 44, 72]. The power-law scattering exponent, p = 4, in q-interval of $0.2 - 0.4$ nm^{-1} points to smooth surface of fullerene aggregates.

Double dilution of the initial solution I by toluene results in cluster state reorganization. Namely, the change of the power-law exponent from p = 4 to p = 2.4 (red line on Figure 9) corresponds to the occurrence of branched clusters with fractal dimension $D_m = p = 2.4$ (mass fractal). It should be noted that the fractal dimension of fullerene clusters in non-polar

solvents, is in general within the range 1.8–3 and depends on fullerene concentration [35] or/and on method of preparation [11, 37, 60]. Correlation between fullerene concentration and some aggregates structural parameters, such as size and fractal dimension, should be highlighted. At a higher concentration of C_{60} in solution, a greater number of monomers is present in the given volume of the solvent. Thus, a bigger number of C_{60} (and C_{60} oxides) are involved in the first stages of self-assembly, which leads to an increase in the geometric size of the aggregates. The higher concentration of monomers leads to increase in fractal dimension due to an aggregation process via monomer – cluster interaction (common for initial stages of cluster growth), which produces denser clusters in comparison to cluster – cluster aggregation (common for later stages). It becomes evident, that the later type of aggregation becomes essential for less concentrated fullerene solutions.
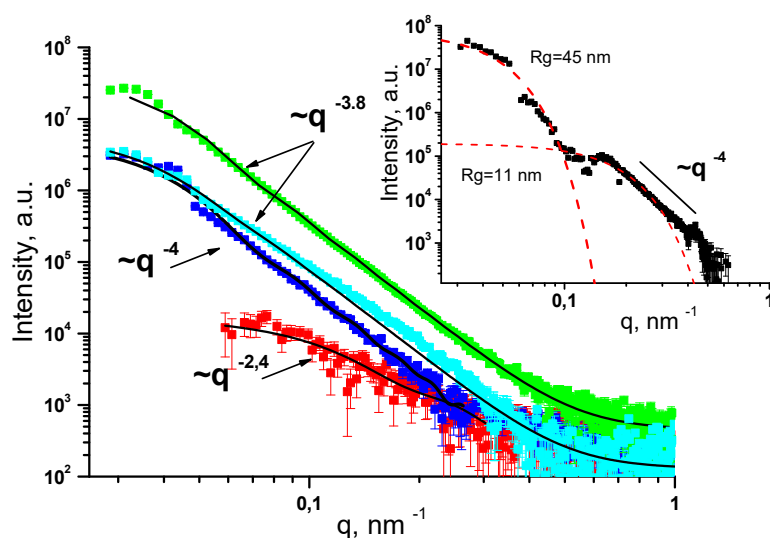

Figure 9. Experimental X-ray scattered intensity curves (colored points) for the C_{60} in toluene solution (red) and in toluene-acetonitrile mixtures with v/v ratio 7:3 (green), 3:2 (blue), 1:1 (dark blue) at fullerene concentration 1.9×10^{-3} M. The black solid lines correspond to the model curves obtained using the IFT procedure. A specific power-law type scattering regimes are also denoted. Inset shows the SAXS curve of the initial C_{60} solution in toluene with

fullerene concentration 3.8×10^{-3} M (stock solution I). The red dashed lines display the contributions of two scattering levels (bi-modal cluster distribution) to I(q).

[**Figure 9** near here]

A different by character structural reorganization takes place when stock solution I is dissolved by toluene-acetonitrile mixtures in a way that the volume ratios of nonpolar and polar solvents were 7:3, 3:2, 1:1 (by volume). In comparison with the C_{60} solution in toluene, where $Rg = 15.9 \pm 0.5$ nm, the addition of acetonitrile leads to the formation of the larger aggregates with Rg values 49.9 ± 0.1 nm, 51.1 ± 0.3 nm and 52.2 ± 0.2 nm for solutions with the v/v ratios 7:3, 3:2 and 1:1, respectively. Along with this, the power-law scattering of the mixtures with exponents $p = 3.8$ and $p = 4$ reflects the more close-packed structure of aggregates in comparison with toluene C_{60} solution at the same fullerenes concentration.

3.6. SANS study of oversaturated C_{60} solutions in toluene–acetonitrile mixed solvent

The structure of aggregates in the mixtures with lower fullerene concentration was investigated by small-angle neutron scattering (SANS). The stock solution II with concentration 4.58×10^{-4} M was prepared in the same way. The scattering signal from two-times diluted system and toluene-acetonitrile mixtures are presented on Figure 10. The maximum aggregate size detected is limited by the instrumental q-range in this case and is more than D $> 2\pi \cdot q_{min}^{-1} \approx 90$ nm. Due to the lack of the Guinier regime the SANS curves were approximated by the power-law function. The obtained power-law scattering exponent for solution C_{60} in toluene reflects a branched structure of aggregates and corresponds to mass fractal with Dm = 1.5. Further, as shown on Figure 10, with increase of acetonitrile fraction in binary mixtures the structure of aggregates gets denser. However, the power-law scattering exponents are less than 3 for all curves, that is, the aggregates structure still corresponds to

mass fractal. Thus, SANS data confirm that an increase in the polar component in the mixtures leads to formation of more compact fullerene aggregates. Considering the results mentioned above, it can be concluded that the aggregates structure in a toluene solution strongly depends on the fullerene concentration.
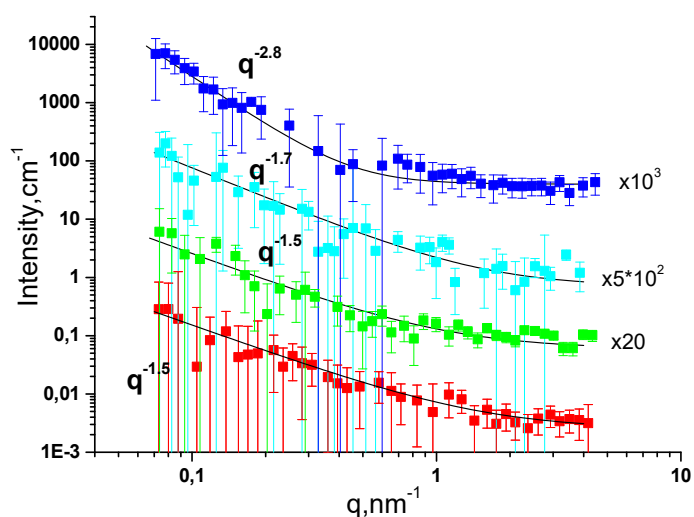

Figure 10. Experimental small-angle neutron scattered intensity curves (colored points) for the C_{60} in toluene solution (red) and toluene-acetonitrile mixtures with v/v ratio 7:3 (green), 3:2 (blue), 1:1 (dark blue). Fullerene concentration is equal to 2.3×10^{-4} M and is the same for all solutions. For clarity, the data were multiplied by factors indicated in the legend. The black solid lines correspond to the model. A specific power-law type scattering regimes are also denoted.

[**Figure 10** near here]

The SANS curves of C_{60} solutions in toluene of different concentrations are presented on Figure 11. One can clearly see an increase in the power-law scattering exponent with increasing of fullerene concentration in the mixtures. An increase in the concentration of

fullerene or the polar component of the mixture leads to the formation of close-packed aggregates, governed mainly by the monomer – cluster aggregation processes.
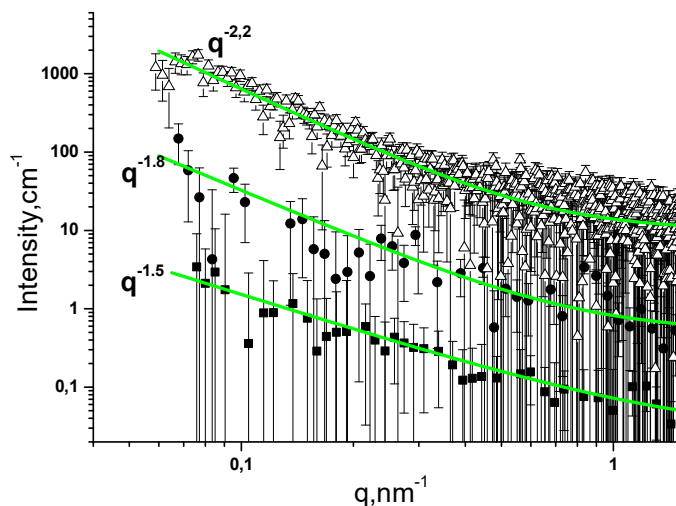

Figure 11. Experimental neutron scattered intensity curves (points) for the C_{60} in toluene solutions with various fullerene concentrations: $2.29{\times}10^{-4}$ M (square), $5.5{\times}10^{-4}$ M (circle) and $1.6{\times}10^{-3}$ M (triangle). For clarity, the curves were shifted vertically. The green solid lines correspond to the power law function. A specific power-law type scattering regimes are also denoted.

[**Figure 11** near here]

3.7. Characterization by DLS techniques of oversaturated fullerene solution prepared in the dark

Prior to the time evolution SAXS experiments, the fullerene C_{60} solutions in toluene - acetonitrile mixtures with v/v ratios 7:3, 3:2, 2:1 were studied by dynamic light scattering. The measurements were carried out 5 min, 3 h, 21 h and one month after samples preparation. All the samples were stable with time and precipitation was not observed visually. This fact

indicates a stabilization mechanism, the formation of a solvate toluene shell around fullerene aggregates being one of the candidates.

The DLS measurement of the initial C_{60} solution in toluene (stock solution III) revealed correlation function corresponding to a monomer solution. It should be noted that stock solution III was prepared without any exposure to light. As shown in Figure 12 the dilution of the stock solution III by toluene-acetonitrile mixtures leads to aggregates formation within 5 min. Earlier it was shown that the growth of fullerene aggregates was detected within 1 h in a mixture of benzene-acetonitrile with concentration 4×10^{-5} M. [14]. Therefore the rate of aggregates growth in mixtures of polar/nonpolar solvents correlates with the fullerene concentration. Furthermore, changes of the cluster size are observed within 21 hours and even further (Figure 12). After 5 min the size distribution functions of the 7:3 and 3:2 (by volume) mixtures reveal two populations of aggregates, with peaks at 34 nm and 16 nm (small-sized aggregates) and at 285 nm and 184 nm, respectively (Figure 12a and b). For both solutions, the populations of small aggregates prevail over the populations of large aggregates (by number). With time the process of narrowing of the cluster size distribution function is observed. This effect is common for various colloidal systems and is explained by the process of continuous detachment / attachment of monomers (single molecules) from the clusters in solution. In the case of a mixture with a maximum fraction of acetonitrile, the situation is somewhat different. On the initial stages the DLS data of 1:1 (by volume) mixture reveal the monomodal distribution of fullerene aggregates, with time evolution of the size. Finally, after one month, the size distribution function shows a wide peak of about 100 nm and an additional low-intensity peak at 350 nm. Thus, apparently, at the first stage, the fraction of toluene is insufficient for the formation of a solvate shell around monomers or small aggregates, which causes a strong association of fullerenes. Then, after a month, as a result of

cluster-cluster interaction the presence of bigger aggregates (second peak at 350 nm) is observed.
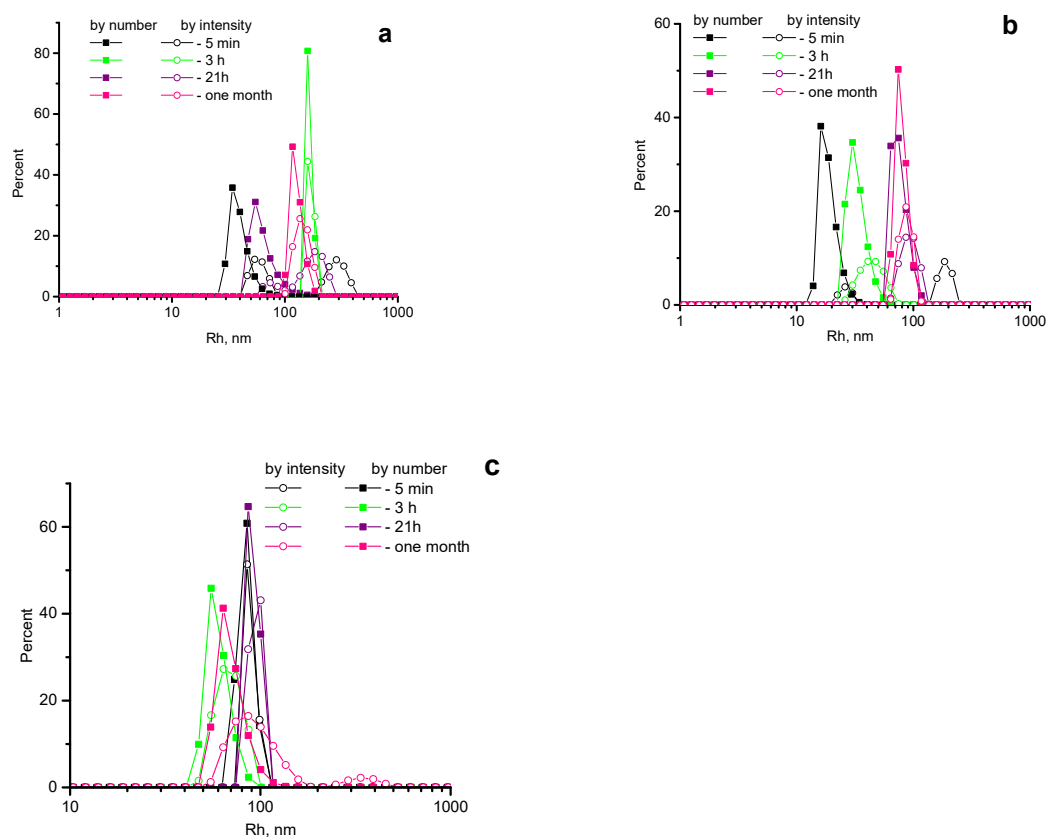

Figure 12. The size distribution by intensity (circle) and by number (square) from DLS measurements of C_{60} solutions in toluene–acetonitrile mixtures with v/v ratio 7:3 (a), 3:2 (b), 2:1 (c) after 5 min (black), 3 h (green), 21 h (purple) and one month (pink). Fullerene concentration 5.5×10^{-4} M is the same for all solutions.

[**Figure 12** near here]

3.8. Time-evolution SAXS studies of oversaturated fullerene solution prepared in the dark

SAXS studies of the fullerene C_{60} solutions in toluene – acetonitrile mixtures with time are presented on Figure 13. The SAXS on C_{60} solution in toluene has a low intensity that is typical for a monomer fullerene solution. For all mixtures, the lack of the Guinier regime

indicates that the maximum aggregate size exceeds 142 nm. This confirms the presence of the large particles, as was obtained by DLS. As can be seen from the Figure 12 for 7:3 (v/v) mixture the scattering intensity starts to exhibit an upturn at approximately $q \approx 0.36$ nm^{-1}, while these points for 3:2 and 2:1 (v/v) mixtures are near 0.28 nm^{-1} and 0.2 nm^{-1}, respectively. This indirectly indicates that the aggregates size is bigger in the mixtures with higher fraction of acetonitrile. Also a slight shift of the SAXS curves with time in Figure 13b, and c has a similar nature, namely an increase in the size of aggregates with time and is in agreement with the DLS data (Figure 12b and c). Especially interesting in the data was the fact that there are no changes of the SAXS curves for mixtures with v/v ratio 7:3 (Figure 12a). The mixture has the least amount of acetonitrile among the systems under study and, apparently, the process of cluster aggregation occurs with lesser intensity. Meanwhile the average size, as well as aggregates structure, remains almost unchanged during the first 3 hours (SAXS measurement time). According to DLS data (black curves on Figure 11a), indeed, the mixture is characterized by wide polydispersity in size from 30 nm up to 100 nm (by number) with peak at 39 nm and from 200 to 450 nm (by intensity), and after changes of structure the average condition would present a similar SAXS profile.
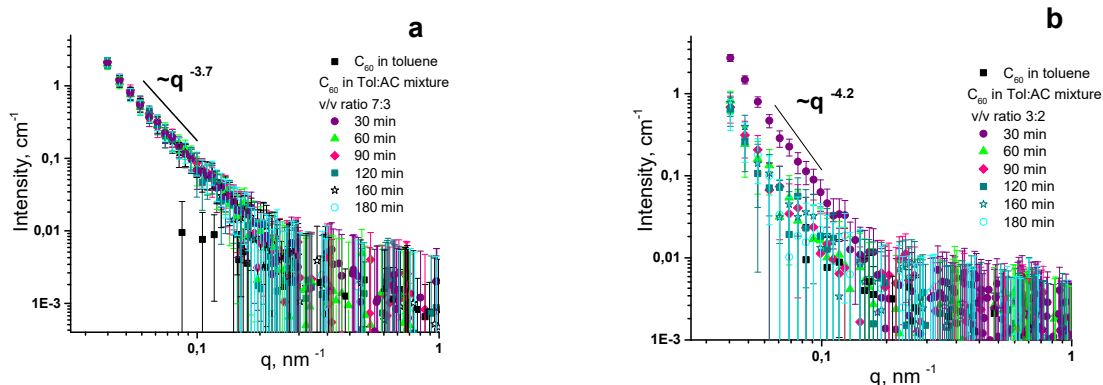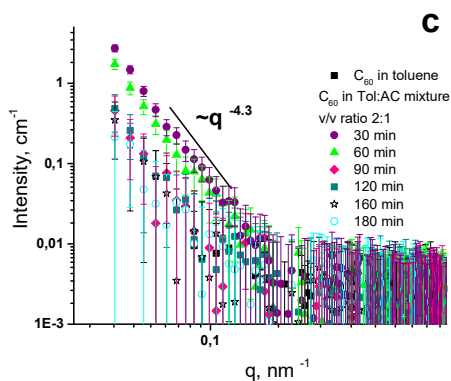
Figure 13. Experimental X-ray scattered intensity curves (colored points) for the C_{60} in toluene solution (black square) and in toluene-acetonitrile mixtures with v/v ratio 7:3 (a), 3:2 (b), 1:1 (c). A specific power-law type scattering regimes are also denoted. Fullerene concentration 5.5×10^{-4} M is the same for all solutions.

[**Figure 13** near here]

The result of a change of the power-law scattering exponent with an increase in acetonitrile fraction in mixtures is quite interesting. As can be seen from Figure 12a, the scaling exponent p = 3.7 indicates the formation of surface fractals in mixture with v/v ratio 7:3. Consequently, at first several fullerene molecules stick together, forming compact small clusters, which are subsequently the core of the monomer – aggregate interaction and, as a result, form surface fractals. For mixtures with a greater fraction of the polar component, the scaling exponent reaches 4.2 and 4.3 (Figure 13b and 13c), that correspond to dense clusters with so-called diffusive interface (p > 4) [73]. This means that in the presence of a dense fullerene core, the scattering length density (SLD) of a cluster surface layer differs from SLD of the core (fullerene) and solvent [74, 75]. This situation can be realized in two cases. In the first case, the particles have a sharp interface, and the solvent cannot penetrate the particle, but the particles themselves have an inner inhomogeneous distribution of SLD from the core to the surface. In another case, the penetration of the solvent into the surface layer of the

29

aggregate is observed. Unlike the surface fractal, the diffuse surface has a denser packing with a small fraction of the solvent inside. According to SAXS data, the formation of dense aggregates with a diffuse surface is observed in the first 30 min after the acentonitrile addition. Further, the size distribution of aggregates changes, while the structure is maintained.

It was previously shown that exposure to light can be the main cause of fullerene aggregation in aromatic solvents [60]. In the work of Makhmanov [37] the fullerene C_{60} aggregates were revealed in toluene solutions prepared by either equilibrium or non-equilibrium methods. Our small-angle data confirm that exposure to light leads to the formation of aggregates in toluene, the stabilization of which probably occurs due to the formation of a solvation shell of an aromatic solvent around fullerenes. The addition of acetonitrile leads to disruption of the solvation shell and a sharp occurrence of aggregation by cluster-cluster and monomer-cluster interaction. As a result, the formation of surface fractals or close-packed aggregates with a smooth surface is observed, depending on the fraction of the polar component in the system (Figure 14). The addition of acetonitrile to the monomeric solution of C_{60} in toluene, prepared in the dark, leads to monomer-monomer aggregation and the formation of aggregates with a diffuse surface, the growth of which is observed over a month. Compaction of the structure and growth of aggregates with increasing concentration of fullerenes or a fraction of a polar solvent is a common property for fullerene solutions under study.
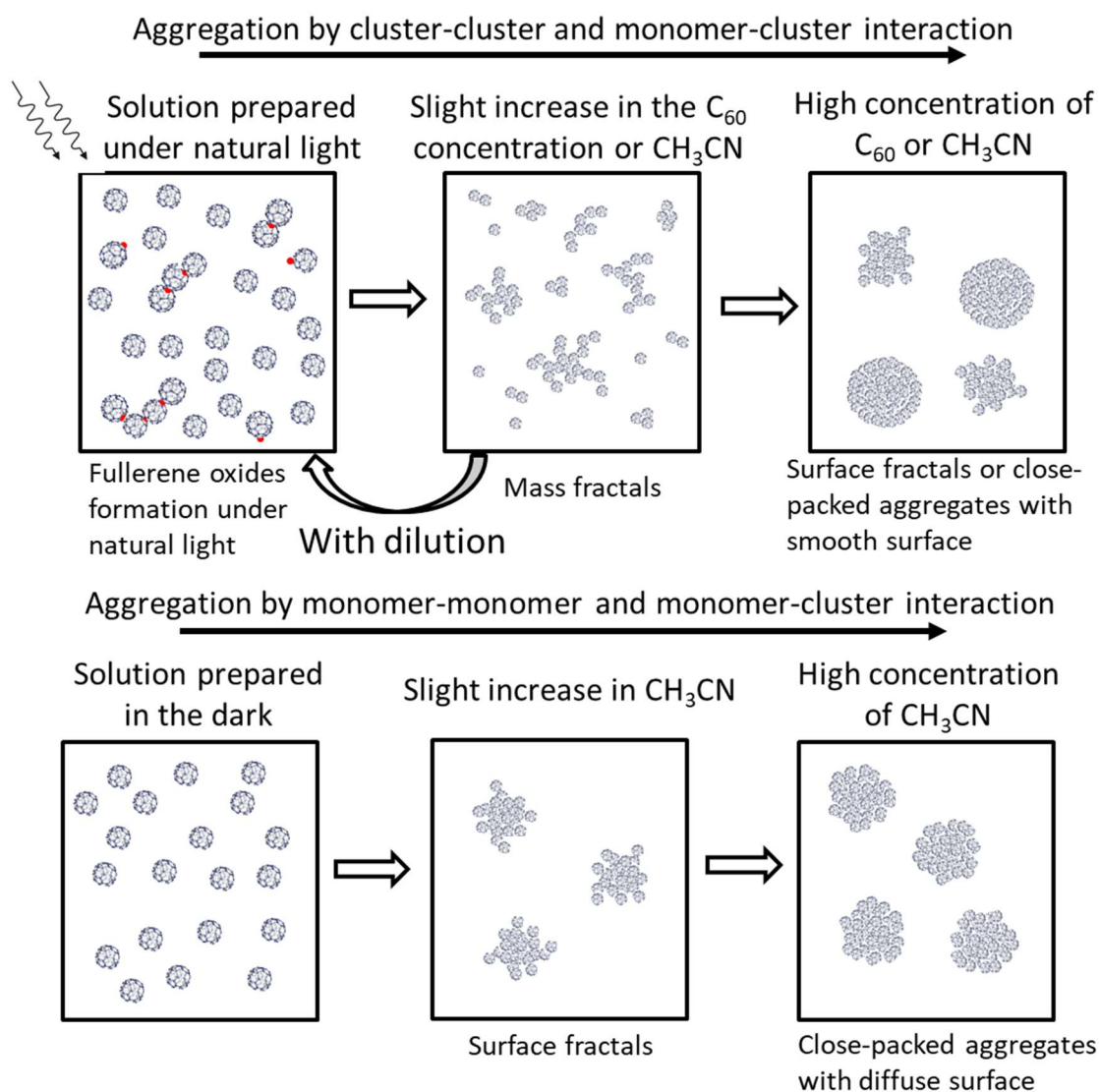
Aggregation by cluster-cluster and monomer-cluster interaction

Solution prepared under natural light

Slight increase in the C_{60} concentration or CH_3CN

High concentration of C_{60} or CH_3CN

Fullerene oxides formation under natural light

Mass fractals

With dilution

Surface fractals or close-packed aggregates with smooth surface

Aggregation by monomer-monomer and monomer-cluster interaction

Solution prepared in the dark

Slight increase in CH_3CN

High concentration of CH_3CN

Surface fractals

Close-packed aggregates with diffuse surface

Figure 14. Schematic representation of aggregation processes in fullerene solutions.

[**Figure 14** near here]

4. Conclusions

Two fundamentally different methods were applied for studying C_{60} organosols in the toluene–acetonitrile binary mixtures. Low-concentrated C_{60} solutions were prepared by dilution of the fullerene solutions in toluene, either saturated or of concentrations below the

solubility limit that is ca. 4×10^{-3} M. Otherwise, the substantially oversaturated stock solutions in toluene were prepared by non-equilibrium methods.

In diluted fullerene systems with concentrations of $(4.0–6.3) \times 10^{-6}$ M, the turning-point from molecular to colloidal solutions depends not only on the mixed solvent composition but also on the fullerene concentration. The system under study follows the Volmer rule: the increase in the acetonitrile content, which lowers the C_{60} solubility, results in decrease of the size of colloidal particles. However, even in acetonitrile-rich media, where fullerene is present in the colloidal state, the UV-visible spectrum retains some features of the molecular absorption. This confirms the idea of formation of the large solvation shells of toluene molecules around fullerenes.

The known tendency of fullerenes to form negatively charged species under contact with acetonitrile was confirmed via the LDI measurements. On the other hand, determinations of the zeta-potential stated that the expressed overcharging of the colloidal particles by multi-charged inorganic cations is a universal property of C_{60} dispersed in polar organic solvents.

The differences between the colloidal solutions of C_{60} prepared in acetonitrile by either 100-fold dilution of the toluene solution or hand-grinding of the solid are most pronounced in the TEM images of dried samples. A distinct enough peculiarity exhibits the UV-visible spectra, whereas the particle size distributions are similar.

The absorption spectra of diluted C_{60} solutions in toluene show no noticeable amounts of fullerene oxides, though the LDI-ToF mass spectra allow revealing some small quantities of $C_{60}O$. After prolonged exposure in air on a steel support, the products of interaction with oxygen were observed, which mainly disappear after washing up by toluene and repeating the mass-spectrometry analysis.

The DLS studies of concentrated solutions of C_{60} in toluene, with concentrations of $(0.23-1.9) \times 10^{-3}$ M, prepared either under natural light or in the dark, confirm that aggregation

occurs as a result of exposition to light and with access to air. It was shown that if the neat filtered solution is sealed and kept in the dark, no clusters are formed within a few weeks. This result is an indication of oxidation processes playing a role in fullerene aggregation in low-polar solvents. This observation is in line with previous reports [60]. Structural SAXS studies of these fullerene solutions indicate the formation of polydisperse aggregates, the size and packing density of which depend on the initial C_{60} concentration. The aggregates are unstable with respect to dilution with toluene and are destroyed, passing to a loose structure. Addition of the polar solvent, acetonitrile, results in structural changes due to cluster-cluster and monomer-cluster interactions. These changes occur rapidly within the first few minutes after dilution, and proceed during a month. As a result, an increase in the size together with compaction of aggregates structure is observed; in the end, the aggregates with a smooth surface and a size of more than 130 nm are present in the system. Another type of aggregate surface is formed in a fullerene solution in toluene-acetonitrile mixture prepared without exposure to light. In this case, at the initial stage aggregation takes place only via monomer-monomer interaction, which leads to the formation of dense aggregates with a diffuse surface, according to SAXS data. Thus, the presence of fullerene oxides in toluene solution affects the structure of aggregates in the system.

References

1. Beck, M.T. Solubility and molecular state of C_{60} and C_{70} in solvents and solvent mixtures. *Pure Appl. Chem.* **1998,** 70, 1881–1887. http://dx.doi.org/10.1351/pac199870101881

2. Semenov, K.N.; Charykov, N.A.; Keskinov, V.A.; Piartman, A.K.; Blokhin, A.A.; Kopyrin, A.A. Solubility of Light Fullerenes in Organic Solvents. *Journal of Chemical & Engineering Data*, **2010**, 55, 13-36. DOI 10.1021/je900296s.

3. Mchedlov-Petrossyan, N.O. Fullerenes in Liquid Media: An Unsettling Intrusion into the Solution Chemistry. *Chemical Reviews*. **2013**, 113, 5149–5193. http://dx.doi.org/10.1021/cr3005026.

4. Rudalevige, T.; Francis, A.H.; Zand, R. Spectroscopic Studies of Fullerene Aggregates. *J. Phys. Chem. A*, **1998**, 102, 9797–9802. http://dx.doi.org/10.1021/jp9832591.

5. Sun, Y.-P.; Bunker, C.E. C_{70} in solvent mixtures. *Nature*, **1993**, 365, 398. https://doi.org/10.1038/365398a0.

6. Sun, Y.-P.; Bunker, C.E. Formation and Properties of C_{70} Solidlike Species in Room-Temperature Solutions. *Chem. Mater*. **1994**, *6*(5), 578-580. https://doi.org/10.1021/cm00041a004.

7. Sun, Y.-P.; Ma, B.; Bunker, C.E.; Liu, B. All-Carbon Polymers (Polyfullerenes) from Photochemical Reactions of Fullerene Clusters in Room-Temperature Solvent Mixtures. *J. Amer. Chem. Soc.* **1995**, 117, 12705–12711. http://dx.doi.org/10.1021/ja00156a007.

8. Nath, S.; Pal, H.; Sapre, A.V. Effect of solvent polarity on the aggregation of C60. *Chem. Phys. Lett.* **2000**, 327, 143–148. http://dx.doi.org/10.1016/S0009-2614(00)00863-0.

9. R.G. Alargova, S. Deguchi, K. Tsujii, Stable Colloidal Dispersions of Fullerenes in Polar Organic Solvents, J. Amer. Chem. Soc., 123 (2001) 10460–10467. http://dx.doi.org/10.1021/ja010202a.

10. M. Alfè, B. Apicella, R. Barbella, A. Bruno, A. Ciajolo, Aggregation and interactions of C60 and C70 fullerenes in neat N-methylpyrrolidinone and in N-

methylpyrrolidinone/toluene mixtures, Chem. Phys. Lett., 405 (2005) 193–197. http://dx.doi.org/10.1016/j.cplett.2005.02.030.

11. O.A. Kyzyma, T.O. Kyrey, M.V. Avdeev, M.V. Korobov, L.A. Bulavin, V.L. Aksenov, Non-reversible solvatochromism in N-methyl-2-pyrrolidone/toluene mixed solutions of fullerene C_{60}, Chem. Phys. Lett., 556 (2013) 178–181. http://dx.doi.org/10.1016/j.cplett.2012.11.040.

12. M. Fujitsuka, H. Kasai, A. Masuhara, S. Okada, H. Oikawa, H. Nakanishi, A. Watanabe, O. Ito, Laser Flash Photolysis Study on Photochemical and Photophysical Properties of C60 Fine Particle, Chem. Letters, 26 (1997) 1211–1212. http://dx.doi.org/10.1246/cl.1997.1211.

13. N.O. Mchedlov-Petrossyan, N.N. Kamneva, Y.T.M. Al-Shuuchi, A.I. Marynin, O.S. Zozulia, A.P. Kryshtal, V.K. Klochkov, S.V. Shekhovtsov, Towards better understanding of C_{60} organosols, Phys. Chem. Chem. Phys., 18 (2016) 2517–2526. http://dx.doi.org/10.1039/C5CP06806A.

14. N.O. Mchedlov-Petrossyan, N.N. Kamneva, Y.T.M. Al-Shuuchi, A.I. Marynin, S.V. Shekhovtsov, The peculiar behavior of fullerene C_{60} in mixtures of 'good' and polar solvents: Colloidal particles in the toluene–methanol mixtures and some other systems, Colloids and Surfaces A: Physicochemical and Engineering Aspects, 509 (2016) 631–637. http://dx.doi.org/10.1016/j.colsurfa.2016.09.045.

15. N.O. Mchedlov-Petrossyan, N.N. Kamneva, Y.T.M. Al-Shuuchi, A.I. Marynin, O.S. Zozulia, Formation and ageing of the fullerene C_{60} colloids in polar organic solvents, J. Mol. Liq., 235 (2017) 98–103. http://dx.doi.org/10.1016/j.molliq.2016.10.113.

16. S. Deguchi, S.-a. Mukai, Top-down Preparation of Dispersions of C_{60} Nanoparticles in Organic Solvents, Chemistry Letters, 35 (2006) 396-397. DOI 10.1246/cl.2006.396

17.   N. O. Mchedlov-Petrossyan, Y. T. M. Al-Shuuchi, N. N. Kamneva, A. I. Marynin, A. P. Kryshtal. Properties of the fullerene C_{60} colloid solutions in acetonitrile as prepared by Deguchi's hand-grinding method. Kharkov University Bulletin. Chemical Ser. (2015) No. 25, 5-11.

18.   T.N. Blanton, C.L. Barnes, M. Lelental, J. Appl. Crystallogr. 33 (2000) 172–173.

19. D. Franke, A.G. Kikhney, D.I. Svergun, Automated acquisition and analysis of small angle X-ray scattering data. Nuclear Instruments and Methods in Physics Research Section A: Accelerators, Spectrometers, Detectors and Associated Equipment 689 (2012) 52–59. https://doi.org/10.1016/j.nima.2012.06.008

20. Glatter, O. (1977) A new method for the evaluation of small-angle scattering data. J. Appl. Cryst. 10, 415–421. https://doi.org/10.1107/S0021889877013879

21. Pedersen, J. S. (1997) Analysis of small-angle scattering data from colloids and polymer solutions: modeling and least-squares fitting. Adv. Coll. Interface Sci. 70, 171–210. https://doi.org/10.1016/S0001-8686(97)00312-6

22.   Kuklin, A. I.; Islamov, A.Kh.; Gordeliy, V. I. Two-detector system for small-angle neutron scattering instrument. *Neutron News* **2005**, *16*, 16−18. https://doi.org/10.1080/10448630500454361

23.   Soloviev, A. G.; Solovieva, T. M.; Stadnik, A. V.; Islamov, A. H.; Kuklin, A. I. The upgrade of package for preliminary treatment of small-angle scattering spectra. JINR Commun. 2003, 10, 2003−2086.

24.   A. Törpe, D. J. Belton. Improved spectrophotometric analysis of fullerenes C60 and C70 in high-solubility organic solvents. Anal. Sci. 31 (2015) 125–130. DOI: 10.2116/analsci.31.125

25. Cataldo F., Iglesias-Groth S., Hafez Y. On the molar extinction coefficients of the electronic absorption spectra of C_{60} and C_{70} fullerenes radical cation. *Eur. Chem. Bull.* **2013**, *2*(12),1013-1018. DOI: http://dx.doi.org/10.17628/ecb.2013.2.1013-1018

26. Ginzburg B.M., Tuĭchiev Sh., Shukhiev S. Permittivity of Low_Concentration C60 Fullerene Solutions in *p_Xylene*. *Tech. Phys. Lett.* **2009**, *35*(6), 491-493.

27. Ginzburg B.M., Tuichiev Sh., Rashidov D., Sodikov F.H., Tabarov S.H., Shepelevskii A.A. Step-Wise Concentration Influence of Fullerenes C_{60} and C_{70} on the Various Parameters of Condensed Systems. Part 1: The Concept of Step-Wise Behavior and its Manifestation in Fullerene Solutions. *J. Macromol. Sci., Part B: Physics*. **2015**, *54*, 533-543.

28. N. V. Mekalova. Fullerenes in Solutions. Ufa State Oil Techn. Univ., Ufa, Russia, 2001, 107 p. (in Russian).

29. Ginzburg B.M., Tuĭchiev Sh. Variations in the structure of aromatic solvents under the influence of dissolved fullerene C_{70}. *Crystallogr. Rep.* **2008**, *53*(4), 645-650.

30. Ginzburg, B. M.; Tuĭchiev, Sh.; Tabarov, S. Kh. Effect of C_{60} Fullerene on the Boiling Point of Its Solutions in Some Aromatic Solvents. *Russ. J. Appl. Chem.* **2009**, *82*(3), 387–390.

31. E. B. Stukalin, M. V. Korobov, N. Y. Avramenko. Solvation free energies of the fullerenes C60 and C70 in the framework of polarizable continuum model. J. Phys. Chem. B. 193 (2003) 9692-9700. https://doi.org/10.1021/jp034567o

32. Peerless, J. S.; Bowers, G. H.; Kwansa, A.L.; Yingling, Y.G. Effect of C_{60} adducts on the dynamic structure of aromatic solvation shells. *Chem. Phys. Lett.* **2017**, *678*, 79–84. https://doi.org/10.1016/j.cplett.2017.04.010

33.   K. Yu. Khanchych, V. P. Zhelezny, I. V. Motovoy, K. F. Tumburkat. The effect of fullerene C_{60} additives on the density of o-xylene. Physics of aerodispersed system. (2019) No. 57, 54-63. http://doi.org/10.18524/0367-1631.2019.57.191953.

34.   M. V. Korobov, E. B. Stukalin, A. L. Mirakyan, I. S. Neretin, Yu. L. Slovokhotov, A. V. Dzyabchenko, A. I. Ancharov, B. P. Tolochko. New solid solvates of C60 and C70 fullerenes: The relationship between structures and lattice energies. Carbon 2003, 41(14):2743-2755. 10.1016/S0008-6223(03)00379-8

35.   R.-H. Guo, C.-C. Hua, P.-C. Lin, T.-Y. Wang, S.-A. Chen, Mesoscale aggregation properties of C_{60} in toluene and chlorobenzene, *Soft Matter*, 12 (2016) 6300-6311. DOI 10.1039/C6SM00602G

36.   Aksenov V.L., Avdeev M.V., Tropin T.V., Priezzhev V.B., Schmelzer J.W.P. Cluster growth and dissolution of fullerenes in non-polar solvents. *J. Mol. Liquids*. **2006**, *127*, 142-144. https://doi.org/10.1016/j.molliq.2006.03.038

37.   Makhmanov, U.; Ismailova, O.; Kokhkharov, A.; Zakhidov, E.; Bakhramov, S. Features of self-aggregation of C_{60} molecules in toluene prepared by different methods. *Phys. Lett. A.* **2016**, *380*, 2081–2084. https://doi.org/10.1016/j.physleta.2016.04.030

38.   Makhmanov, U. K.; Ismailova, O.B.; Kokhkharov, A. M.; Bakhramov, S.A. Analysis of clusterization of C_{70} molecules in benzene solutions prepared by various methods. *Bull. Nat. Univ. Uzbekistan*, **2018**, *1*, 66–72.

39.   Bakhramov, S.; Kokhkharov, A.; Makhmanov, U. The semiconductor films of fullerene C70 nanoaggregates on the surface of a plane glass substrate. *Applied Solar Energy,* **2018**, *54*, 164–167. https://doi.org/10.3103/S0003701X18030052

40.   Makhmanov, U.; Kokhkharov, A.; Bakhramov, S. Organic fractal nano-dimensional structures based on fullerene C_{60}. *Fullerenes, Nanotubes and Carbon Nanostructures.* **2019**, *27*, 273–278. https://doi.org/10.1080/1536383X.2019.1570922

41.　Makhmanov, U. K.; Kokhkharov, A. M.; Bakhramov, S. A.; Erts, D. The formation of self-assembled structures of C_{60} in solutions and in the volume of an evaporating drop of a colloidal solution. *Lithuan. J. Phys.* **2020**, *60*, 194–204. https://doi.org/10.3952/physics.v60i3.4306

42.　M.V. Avdeev, V.L. Aksenov, T.V. Tropin, Models of cluster formation in solutions of fullerenes, Russ. J. Phys. Chem. A, 84 (2010) 1273–1283. http://dx.doi.org/10.1134/S0036024410080017.

43.　Ying, Q.; Marecek, J.; Chu, B. Solution behavior of buckminsterfullerene (C_{60}) in benzene. J. *Chem. Phys.* **1994**, *101*, 2665–2672. https://doi.org/10.1063/1.467646

44.　G. Török, V.T. Lebedev, L. Cser, Small-angle neutron-scattering study of anomalous C_{60} clusterization in toluene, Phys. Solid State, 44 (2002) 572–573. http://dx.doi.org/10.1134/1.1462711.

45.　McElvany, S. W.; Ross, M.M.; Callahan, J. H. Characterization of fullerenes by mass-spectrometry. *Acc. Chem. Res.* **1992**, *25*, 162–168. https://doi.org/10.1021/ar00015a010

46.　Pokrovskiy, V.O.; Grebenyuk, A. G.; Demianenko, E. M.; Kuts, V. S.; Karpenko, O. B.; Snegir, S. V.; Kartel, N. T. Laser desorption/ionization of fullerenes: Experimental and theoretical study. *Chemistry, Physics and Technology of Surfaces*. **2013**, *4*, 78–91.

47.　Henderson, W.; McIndoe, J. S. Mass spectrometric transmission of fullerenes. *Fullerenes, Nanotubes and Carbon Nanostructures*. **2014**, *22*, 663–669. https://doi.org/10.1080/1536383X.2012.717558

48.　Zeegers, G. P.; Günthardt, B.F.; Zenobi, R. Target plate material influence on fullerene-C_{60} laser desorption/ionization efficiency. *J. Amer. Soc. Mass Spectrom*. **2016**, doi: 10.1007/S13361-016-1333-0.

49.   S. W. McElvany, J. H. Callahan, M.M. Ross, L. D. Lamb, D. R. Huffman. Large odd-numbered carbon clusters from fullerene-ozone reactions. Science. 260 (1993) 1632-1634.

50.   S. Lebedkin, S. Ballenweg, J. Gross, R. Taylor, W. Krätschmer. Synthesis of C120O: A bew dimeric [60] Fullerene derivative. Tetrahedron, 36 (1995) 4971-4974.

51. W. A. Scrivens, J. M. Tour, K. E. Creek, Lucia Pirisi , Synthesis of 14C-Labeled C60, Its Suspension in Water, and Its Uptake by Human Keratinocytes. *J. Am.Chem. Soc.*, **116**, 4517-4518 (1994). https://doi.org/10.1021/ja00089a067

52. K. L. Chen, M. Elimelech, Relating Colloidal Stability of Fullerene (C60) Nanoparticles to Nanoparticle Charge and Electrokinetic Properties. *Environ. Sci. Technol.,* **43**, 7270-7276 (2009). https://doi.org/10.1021/es900185p

53.   B.S. Murdianti, J.T. Damron, M.E. Hilburn, R.D. Maples, R.S. Hikkaduwa Koralege, S.I. Kuriyavar, K.D. Ausman. C_{60} Oxide as a Key Component of Aqueous C_{60} Colloidal Suspensions Environ. Sci. Technol. 2012, 46, 7446−7453 DOI: 10.1021/es2036652

54.   L. Pospısil, M. Gal, M. Hromadova, J. Bulıckova, V. Kolivoska, J. Cvacka, K. Novakova, L. Kavan, M. Zukalova, L. Dunsch. Search for the form of fullerene C_{60} in aqueous medium. *Phys. Chem. Chem. Phys.,* 2010, **12**, 14095–14101. **https://doi.org/10.1039/C0CP00986E**

55.   Taylor, R.; Barrow, M.P.; Drewello, T. C_{60} degrades to $C_{120}O$. *Chem. Commun*. **1998**, 2497–2498. **https://doi.org/10.1039/A806726K**

56.   Al-Jafari, M.S.; Barrow, M.P.; Taylor, R.; Drewello, T. Laser-induced gas-phase synthesis of dimeric C_{70} oxides. *Int. J. Mass Spectrom*, **1999**, *184*, L1–L4. https://doi.org/10.1016/S1387-3806(99)00029-9

57.   Barrow, M.P.; Drewello, T. Significant interferences in the post source decay spectra of ion-gated fullerene and coalesced carbon cluster ions. *Int. J. Mass Spectrom*, **2000**, *203*, 111–125. https://doi.org/10.1016/S1387-3806(00)00293-1

58.   Barrow, M.P.; Feng, X.; Wallace, J. I.; Boltalina, O.V.; Taylor, R.; Derrick, P.J.; Drewello, T. Characterization of fullerenes and fullerene derivatives by nanospray. *Chem. Phys. Lett*. **2000**, *330*, 267–274. https://doi.org/10.1016/S0009-2614(00)01124-6

59.   Pace, M. D.; Christidis, T. C.; Yin, J. J.; Milliken, J. EPR of a free radical in C_{60}: Effect of O_2. *J. Phys. Chem*. **1992**, *96*, 6855–6858. https://doi.org/10.1021/j100196a001

60.   Dattani, R.; Gibson, K. F.; Few, S.; Borg, A. J.; DiMaggio, P.A.; Nelson, J.; Kazarian, S. G.; Cabral, J.T. Fullerene oxidation and clustering in solution induced by light. *J. Colloid Interface Sci.* **2015**, *446*, 24–30. https://doi.org/10.1016/j.jcis.2015.01.005

61.   Creegan, K. M.; Robbins, J. I.; Robbins, W. K.; Millar, J. M.; Sherwood, R. D.; Tindall, P. J.; Cox, D. M.; Smith, A. B.; McCauley, J. P.; Jones, D. R.; Gallakher, R. T. Synthesis and characterization of $C_{60}O$, the first fullerene epoxide. *J. Amer. Chem. Soc*. **1992**, *114*, 1103–1105. https://doi.org/10.1021/ja00029a058

62.   R. B. Weisman, D. Heyman, S.M. Bachilo. Synthesis and characterization of the "missing" oxide of C_{60}: [5,6]-open $C_{60}O$. J. Am. Chem. Soc. 2001. 123, 9720–9721. https://doi.org/10.1021/ja016267v

63.   C. Reichardt, T. Welton, Solvents and Solvent Effects in Organic Chemistry, Wiley2011.

64.   M. T. Beck, M. G. Mandi, Solubility of C_{60}. Fullerene Sci. Technol. 2 (1997) 291–310. https://doi.org/10.1080/15363839708011993

65.   M. Volmer. Kinetik der Phasenbildung (Russian translation). Moscow, Nauka, 1986, Ch. 5.

66. N. A. Marfunin, N.O. Mchedlov-Petrossyan. Behavior of fullerene C_{70} in binary organic solvent mixtures as studied using UV-vis spectra and dynamic light scattering. Kharkov University Bull. C(2019) **Вестник Харьковского национального университета**. Серия «Химия». 2019 Вып. 33 (56). С. 77–87. http://doi.org/10.26565/2220-637X-2019-33-06

67. N. O. Mchedlov-Petrossyan, Y. T. M. Al-Shuuchi, N. N. Kamneva, A. I. Marynin, V. K. Klochkov. The Interactions of the nanosized aggregates of fullerene C_{60} with electrolytes in methanol: Coagulation and overcharging of particles. *Langmuir,* 32 (2016) 10065-10072. http://dx.doi.org/10.1021/acs.langmuir.6b02533 .

68. N. O. Mchedlov-Petrossyan, N. N. Kamneva, Y. T. M. Al-Shuuchi, A. I. Marynin. Interaction of C_{60} aggregates with electrolytes in acetonitrile. Colloids and Surfaces A: Physicochemical and Engineering Aspects. 2017. Vol. 516. P. 345-353. http://dx.doi.org/10.1016/j.colsurfa.2016.12.035

69. H. Ohshima, A Simple Expression for Henry's Function for the Retardation Effect in Electrophoresis of Spherical Colloidal Particles, Journal of Colloid and Interface Science, 168 (1994) 269–271. http://dx.doi.org/10.1006/jcis.1994.1419.

70. Tropin, T. V.; Jargalan, N.; Avdeev, M. V.; Aksenov, V. L. Investigations of the kinetics of cluster growth in fullerene C_{60} solutions. *Ukr. J. Phys.* **2020**, *65*, 701–708. DOI: 10.15407/ujpe65.8.701

71. T.V. Tropin, M.V. Avdeev, V.L. Aksenov, Small-angle neutron scattering data on C60 clusters in weakly polar solutions of fullerenes. Crystallography Reports 52 (2007) 483–486. DOI: 10.1134/S1063774507030261

72. S.V. Snegir, T.V. Tropin, O.A. Kyzyma, M.O. Kuzmenko,V.I. Petrenko, V.M. Garamus, M. V. Korobov, M.V. Avdeev, L.A. Bulavin. On a specific state of C60

fullerene in N-methyl-2-pyrrolidone solution: Mass spectrometric study. Applied Surface Science 481 (2019) 1566–1572. DOI: 10.1016/j.apsusc.2019.03.168

73. G. Beaucage, Approximations leading to a unified exponential/power-law approach to small-angle scattering, J. Appl. Crystallogr. 28 (1995) 717–728, https://doi.org/10.1107/S0021889895005292.

74. M.V. Avdeev, V.L. Aksenov, O.V. Tomchuk, L.A. Bulavin, V. M. Garamus, E. Osawa. The spatial diamond–graphite transition in detonation nanodiamond as revealed by small-angle neutron scattering. J. Phys.: Condens. Matter 25 (2013) 445001. DOI: 10.1088/0953-8984/25/44/445001

75. Oleksandr V. Tomchuk, Mikhail V. Avdeev, Aleksandr E. Aleksenskii, Aleksandr Ya. Vul, Oleksandr I. Ivankov, Vasyl V. Ryukhtin, János Füzi, Vasil M. Garamus, and Leonid A. Bulavin. Sol–Gel Transition in Nanodiamond Aqueous Dispersions by Small-Angle Scattering. J. Phys. Chem. C 2019, 123, 29, 18028–18036. https://doi.org/10.1021/acs.jpcc.9b03175